JOBS
مجلة العلوم الأساسية
Journal of Basic Science
Print -ISSN 2306-5249
Online-ISSN 2791-3279
العدد السادس والأربعون
٢٠٢٦م/١٤٤٨هـ
العدد السادس والأربعون
(371)- (351)

إزالة الكبريت من النفط الخام الثقيل بالامتزاز باستخدام دقائق أكسيد النحاس النانوية

م. د. الاء عيسى سلطان
قسم علوم الكيمياء، كلية العلوم، جامعة ديالى
alaesa1988@gmail.com

المستخلص:

يهدف هذا البحث إلى تقييم كفاءة جسيمات أكسيد النحاس النانوية (CuO–NPs) في إزالة المركبات الكبريتية من النفط الخام بطريقة الامتزاز. حُضّرت الجسيمات النانوية باستخدام طريقة السول–جل، ثم شُخّصت باستعمال حيود الأشعة السينية (XRD)، والمجهر الإلكتروني الماسح ذي الانبعاث الميداني (FESEM)، والتحليل الطيفي لتشتت طاقة الأشعة السينية (EDX)، بهدف تحديد بنيتها البلورية وخصائصها المورفولوجية وتركيبها العنصري. أظهرت نتائج XRD قمماً عند زوايا حيود مقدارها ٣١,٦ و٤٥,٤ و٥٦,٤ و٦٦,٣ و٧٥,٢°، نُسبت إلى المستويات البلورية (١١٠) و(١١٢) و(٢٠٢) و(٢٢٠) و(٠٠٤)، على التوالي، واستُخدمت هذه النتائج في توصيف البنية أحادية الميل لجسيمات CuO النانوية. وبلغ متوسط الحجم البلوري المحسوب باستخدام معادلة ديباي–شيرر ٣٤,٦ نانومتر. كما أظهر تحليل FESEM وجود جسيمات متكتلة ذات شكل كروي تقريبي، وتراوحت أحجام الجسيمات المرصودة بين ٤٢,٤٣ و٨٧,٠٩ نانومتر. وأوضح تحليل EDX أن النحاس والأكسجين كانا العنصرين السائدين، بنسبة ٨٠,٦% و١٣,٩%، على التوالي، في حين بلغت نسبة الكربون ٥,٥%، مما يدعم نجاح تكوين جسيمات أكسيد النحاس النانوية. سُجلت أعلى كفاءة لإزالة الكبريت، والبالغة ٣٦,٨٥%، عند درجة حرارة ٢٩٨ كلفن، وباستخدام ٢٥٠ ملغم من CuO–NPs، وزمن تماس مقداره ٥٠ دقيقة. وازدادت كفاءة الإزالة مع زيادة جرعة المادة الممتزة وزمن التماس، في حين انخفضت بارتفاع درجة الحرارة. وتشير هذه النتائج إلى أن جسيمات أكسيد النحاس النانوية تمتلك قابلية واعدة للاستخدام في إزالة المركبات الكبريتية من النفط الخام، مع

JOBS
مجلة العلوم الأساسية
Journal of Basic Science
Print -ISSN 2306-5249
Online-ISSN 2791-3279
العدد السادس والأربعون
٢٠٢٦م/١٤٤٨هـ

الحاجة إلى مزيد من الدراسات المتعلقة بالتحسين، والتوصيف السطحي، والنمذجة الحركية والثرموديناميكية، وتجديد المادة الممتزة قبل التوسع نحو التطبيقات العملية.

الكلمات المفتاحية: الامتزاز؛ جسيمات أكسيد النحاس النانوية؛ إزالة الكبريت؛ النفط الخام؛ طريقة سول–جل.

Removal of Sulfur Compounds from Crude Oil by Adsorption onto Copper Oxide Nanoparticles

Lecturer Dr. Alaa E. Sultan
Department of Chemistry, College of Science. University of Diyala
alaesa1988@gmail.com

Abstract

This research aims to study the efficiency of copper oxide nanoparticles (CuO-NPs) in adsorbing and desulfurizing crude oil. The nanoparticles were prepared using the sol-gel method and characterized using advanced analytical techniques such as XRD, FESEM, and EDX to confirm their crystalline structure, morphology, and elemental composition. XRD results of crystalline planes of reveals peaks at 31.6, 45.4, 56.4, 66.3, and 75.2 that indexed planes (110), (112), (202), (220) and (004), respectively, was used to characterize the monoclinic structure of CuO-NPs with an average size 34.6 nm calculated using Deby-Sherrer equation, FESEM analysis revealed agglomerated spherical particles at different magnifications. Particle sizes ranged from 42.43 to 87.09 nm; EDX data showed Cu (80.6%), O (13.9%), and C (5.5%). The peaks associated with Cu and O provide strong evidence that the nanocrystals are composed of only CuO-NPs. The highest sulfur removal efficiency of 36.85% was obtained at 298 K using 250 mg of CuO-NPs and a contact time of 50 min. Removal efficiency increased with decreasing temperature and increasing adsorbent dosage and contact time. These results confirm that copper nanoparticles are a promising and effective method for sulfur removal compared to conventional methods, with potential for future industrial applications.

JOBS
مجلة العلوم الأساسية
Journal of Basic Science
Print -ISSN 2306-5249
Online-ISSN 2791-3279
العدد السادس والأربعون
٢٠٢٦م/١٤٤٨هـ

Keywords: adsorption; CuO-NPs; desulfurization; crude oil; sol-gel

1. Introduction

Demand for crude oil as a primary energy source continues to rise, driven by economic growth. This has prompted researchers to develop desulfurization technologies to improve crude oil quality and reduce its sulfur content [1,2]. High sulfur levels in crude oil negatively affect refining processes, most notably causing corrosion in pipes and equipment, in addition to environmental damage [3,4]. Heavy crude oil is characterized by properties such as high viscosity, high density, high acidity, and increased sulfur content.

One of the most common industrial methods for desulfurization is hydrodesulfurization (HDS), the most widely used technology in oil refineries to reduce sulfur content to a minimum. However, this method is expensive, requires harsh operating conditions (temperature and pressure), and is ineffective at removing aromatic cyclic sulfur compounds such as thiophene, benzothiophene, and dibenzothiophene [5]. As an alternative to HDS, other methods for sulfur removal have emerged, such as solvent extraction, adsorption, photo-oxidation, and ionic liquids [6,7].

Adsorption is one of the most promising methods because it can use various adsorbent materials, provided the adsorbent has an active surface, a high surface area, and a suitable pore-size distribution [7]. Adsorption technology for sulfur removal depends on the adsorbent's nature and its physical and chemical properties in removing organo-sulfur compounds [8]. Several adsorbent materials have been employed for this purpose, such as activated carbon, Y-type zeolite, and nanomaterials, such as copper oxide nanoparticles.

One major challenge in adsorptive desulfurization is that the high adsorption capacity in model fuels does not necessarily translate into comparable performance in real petroleum streams where aromatic hydrocarbons, nitrogen-containing compounds, resins, and other competitive

species may occupy the same active sites as organosulfur molecules [9]. Thus, sulfur removal depends not only on total surface area but also on pore accessibility, surface chemistry, active-site density, and adsorption selectivity [10]. Hierarchical pore networks with larger transport channels and smaller adsorption pores can improve mass transfer, facilitating diffusion of bulky thiophenic compounds [11]. However, excessive metal loading can block pores, reduce available surface area, and promote particle agglomeration [12]. The oxidation state and coordination environment of the copper sites are also important because Cu species can interact with sulfur compounds via Cu–S coordination, Lewis acid-base interactions, or π-complexation [13]. Heavy crude oil is highly viscous and compositionally complex, which hinders diffusion and prolongs adsorption equilibrium [14]. So, the evaluation of any adsorbent should be based on kinetics, capacity at equilibrium, competitive adsorption and regeneration stability, not only on removal efficiency [15-18].

Recent studies showed that copper-containing adsorbents can act as effective active sites for capturing refractory sulfur compounds from petroleum-derived streams. Hence, Ma et al. prepared a Cu(I)-based adsorbent for selective adsorption of dibenzothiophene, lowering the sulfur concentration from 100 to ~9 mg S L^{-1} in a toluene–isooctane model oil at 298 K. The improved selectivity resulted from strong Cu–S interactions at the molecular scale [13]. Musa et al. prepared Cu, Ni, and Cu–Ni nanoparticles-modified alum sludge for desulfurization of diesel and kerosene. The results showed that metal loading and surface area greatly influenced the performance of the materials. The Cu-Ni-containing material showed the highest efficiency for sulfur removal. The adsorption data also fit the Langmuir model better than the Freundlich and Temkin models [15]. Zhu et al. reported a CuO-impregnated hierarchical porous carbon for ethyl mercaptan removal, in which the 5 wt.% CuO formulation reached breakthrough and saturation sulfur capacities of 165.1 and 222.7 mg g^{-1}, respectively, while it kept 91% of its initial capacity after five regeneration cycles [12]. Altogether, these results show that copper oxidation state,

JOBS
مجلة العلوم الأساسية
Journal of Basic Science
Print -ISSN 2306-5249
Online-ISSN 2791-3279
العدد السادس والأربعون
٢٠٢٦م/١٤٤٨هـ

dispersion, pore architecture, and support choice are key parameters for adsorption efficiency and reusability in desulfurization systems.

Several researchers have studied sulfur removal from various petroleum derivatives using adsorption technology. However, no previous studies have addressed removing organic sulfur compounds from heavy crude oil. This study sheds light on the desulfurization of heavy crude oil extracted from the East Baqubah field, which contains 1.78% sulfur, using adsorption technology using nanocupric oxide. The research also examined the effect of adsorption time and modified matrix concentration on the efficiency of the removal process.

2. Materials and Methods

2.1 Synthesis of copper oxide nanoparticles (CuO-NPs)

The CuO nanoparticles were synthesized in solution using the sol-gel method [$Cu(NO_3)_2.3H_2O$] and citric acid dissolved in ionic water with a concentration of 0.1 M. The solution was stirred on a magnetic stirrer at 90 °C. Agitation continued until gelation was obtained. Afterward, the gel was combusted at 110 °C. The material was also annealed for 4 h at 450 °C to obtain crystalline CuO nanoparticles [19]. The process is shown in Figure 1.

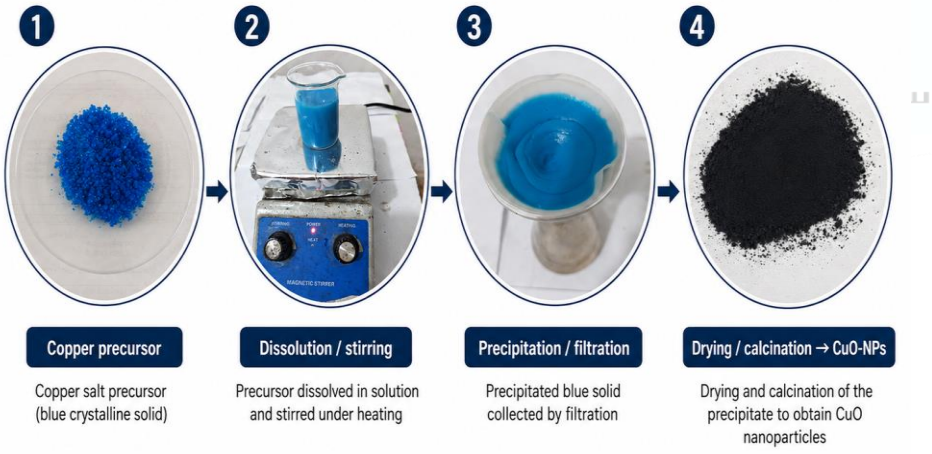

Figure 1. A diagram of the preparation method.

JOBS مجلة العلوم الأساسية
Journal of Basic Science
Print -ISSN 2306-5249
Online-ISSN 2791-3279
العدد السادس والأربعون
٢٠٢٦م/١٤٤٨هـ

2.2 Characterization of CuO-NPs

The synthesized CuO-NPs were characterized by X-ray diffraction (XRD), scanning electron microscopy (SEM), energy dispersive X-ray spectroscopy, and atomic absorption spectroscopy (AAS). The crystalline structure and phase composition were studied by the XRD (Siemens D500, Siemens AG, Germany). The diffractometer was operated with Cu Kα radiation (wavelength =1.54060 Å) at an accelerating voltage of 40 kV and a current of 30 mA. The surface morphology of the nanoparticles was studied by a scanning electron microscope (ZEISS Sigma VP, Carl Zeiss Microscopy GmbH, Germany). The elemental composition was studied by energy-dispersive X-ray spectroscopy using a silicon drift detector (SDD X-Max, Oxford Instruments, UK) attached to the SEM. Concentrations of the measured ionic species were determined using the AA-7000 atomic absorption spectrophotometer (Shimadzu Corporation, Japan) with atomic absorption measurements [20].

2.3 Desulfurization process

The crude oil desulfurization process involved mixing 20 mL of heavy crude oil with CuO-NPs at different concentrations (50, 100, 150, 200, and 250 mg) inside an Erlenmeyer flask. The samples were then ultrasonicated for several periods of time (10, 20, 30, 40, and 50 min) at a constant water temperature of 25 °C. The mixture was then allowed to settle to a slurry, while the treated crude oil was subsequently used for sulfur content analysis.

2.4 Determination of removal rate

The removal percentage (R %) was determined utilizing equations [21, 22].

$$R\% = \frac{(C_o - Ce)}{C_o} \times 100 \ldots\ldots(1)$$

Whereas:
R%: Percentage of sulfur removed from the crude oil.

JOBS مجلة العلوم الأساسية Journal of Basic Science
Print -ISSN 2306-5249
Online-ISSN 2791-3279
العدد السادس والأربعون
٢٠٢٦م/١٤٤٨هـ

C_o: First concentration of metallic ion, expressed in mg/L.
C_e: Concentration of metallic ions post-adsorption (mg/L).

3. Results and Discussion

Different techniques and instruments were used to characterize the Cupper NPs adsorbent. The details were illustrated in the next section.

3.1 X-ray diffraction

The adsorbents were characterized using XRD, and the crystal size was measured with a powder X-ray diffractometer. Cu Kα radiation was utilized (k Cu = 1.5406 Å). The XRD pattern of CuO nanoparticles is shown in Fig. 2. The distinct peaks at 2θ indicate the crystalline nature of CuO nanoparticles. Crystallographic plane analysis confirms peaks at 31.6, 45.4, 56.4, 66.3, and 75.2, indexed to (110), (112), (202), (220), and (004), respectively, which defines the monoclinic structure of CuO-NPs [23, 24]. This is in agreement with five peaks in the XRD pattern, and no other peaks are observed, which reveals the phases of CuO NPs nanostructures [25]. The particle size was calculated by the Debye-Scherrer equation as follows:

$$D = \frac{0.9\,\lambda}{\beta \cos\theta} \ldots\ldots (2)$$

Where:
D: represents the size of crystallite.
λ: represents the wavelength of radiation.
θ: represents Bragg's angle.
β: is the full width at half maximum (FWHM) [26].
The particle size of CuO nanoparticles is determined to be 34.6 nm. The material's nanocrystalline characteristics are evidenced by pronounced peaks in XRD samples and particle sizes less than 100 nm.

JOBS
مجلة العلوم الأساسية
Journal of Basic Science
Print -ISSN 2306-5249
Online-ISSN 2791-3279
العدد السادس والأربعون
٢٠٢٦م/١٤٤٨هـ

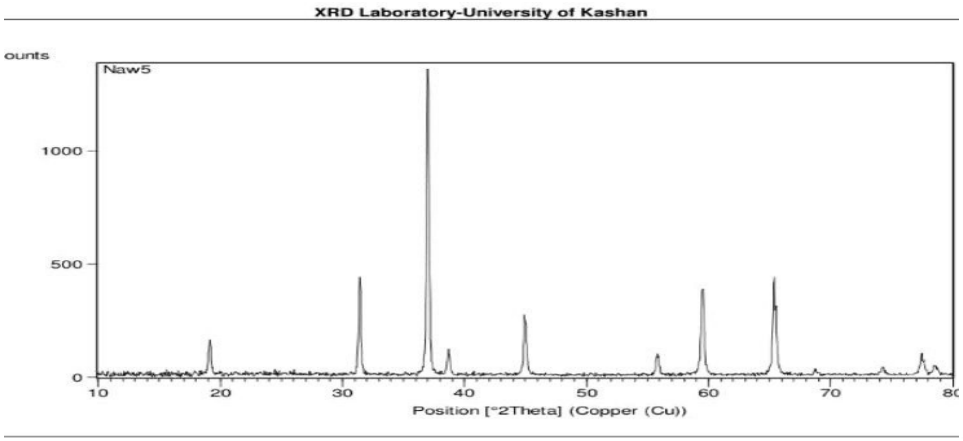

Figure 2. XRD of CuO-NPs synthesis

3.2 Field Emission Scanning Electron Microscopy (FESEM)

FESEM image revealed strongly agglomerated particles with roughly round and irregular shapes. The observed particle size was between 42.43 and 87.09 nm, which was higher than the crystallite size calculated from XRD. This is expected because FESEM measures visible particles or agglomerates, whereas the Debye–Scherrer equation estimates the size of coherent crystalline domains [12]. The observed agglomeration may reduce the number of directly accessible adsorption sites and increase the resistance to the transfer of sulfur-containing molecules through the crude-oil phase. Dispersion of CuO nanoparticles and retention of accessible pore structures are important factors that control sulfur adsorption performance [30]. Hence, the synthesized particles are in the nanoscale range, but their effective adsorption performance might be limited by the incomplete dispersion in the viscous crude-oil matrix [23], as shown in Figure 3.

JOBS
مجلة العلوم الأساسية
Journal of Basic Science
Print -ISSN 2306-5249
Online-ISSN 2791-3279
العدد السادس والأربعون
٢٠٢٦م/١٤٤٨هـ

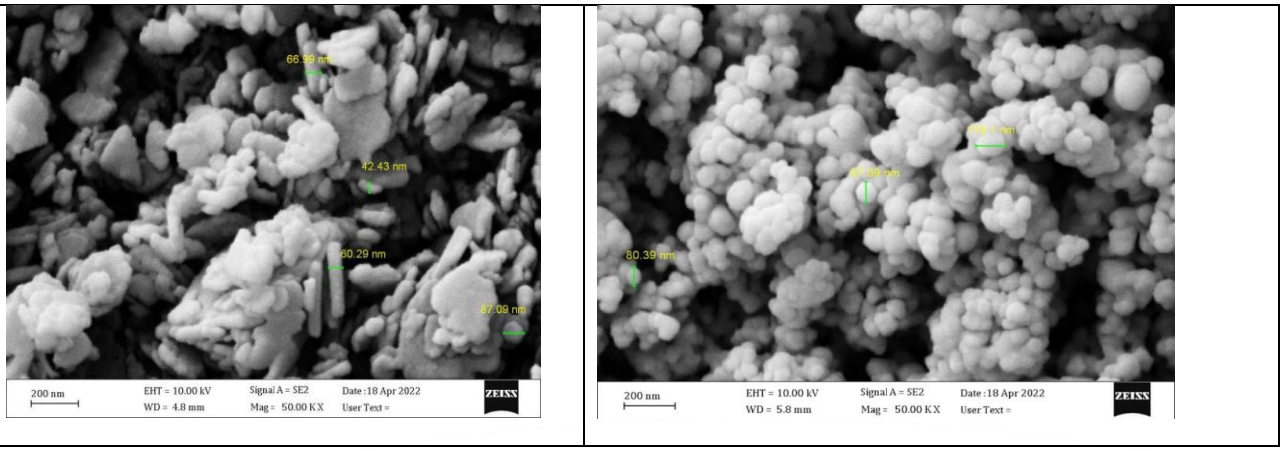

Figure 3. Different views of CuO-NPs using FESEM.

3.3 Energy-dispersive X-ray Analysis Spectroscopy

The elemental composition of the synthesized CuO-NPs was analyzed by EDX, and the obtained spectrum is presented in Figure 4. The dominant elements detected were copper and oxygen (80.6 and 13.9 wt.%, respectively) with carbon (5.5 wt.%). The emergence of intense Cu and O signals confirms the successful formation of a copper oxide-rich nanomaterial, consistent with the elemental composition widely reported for the synthesized CuO-NPs [23,24]. Therefore, the confirmation of the monoclinic CuO phase should be based mostly on the XRD results. The observed carbon signal may arise from the carbon-containing sample support, residual citric acid after synthesis, or adventitious carbon contamination introduced during handling and analysis. The Au peak in the spectrum most likely arises from the conductive gold coating applied before FESEM–EDX examination to increase surface conductivity and reduce charging [28]. Therefore, Au cannot be regarded as an intrinsic constituent of the synthesized nanoparticles.

JOBS
مجلة العلوم الأساسية
Journal of Basic Science
Print -ISSN 2306-5249
Online-ISSN 2791-3279
العدد السادس والأربعون
٢٠٢٦م/١٤٤٨هـ

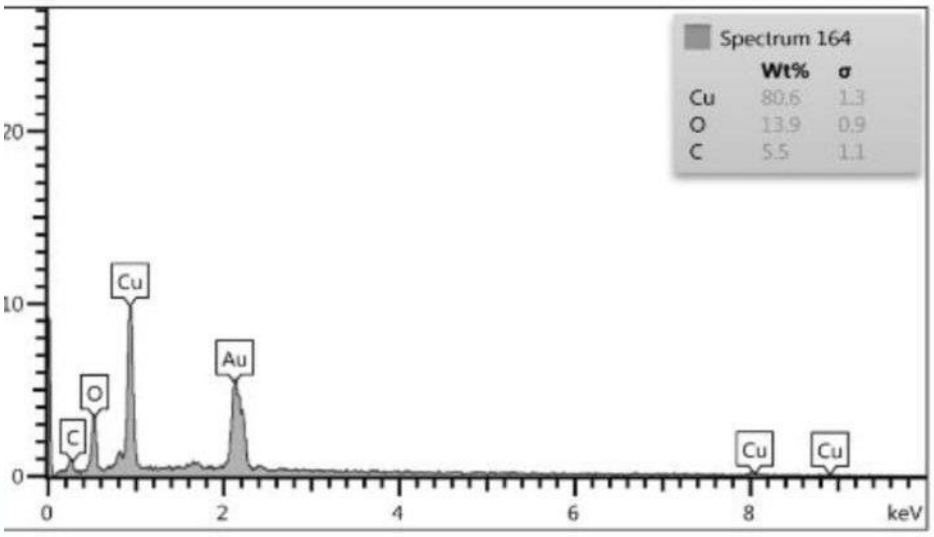

Figure 4. EDXA of CuO-NPs synthesis

3.4 Optimization of conditions

Sulfur removal from crude oil was studied at different time intervals and different concentrations for CuO-NPs to find the best conditions for desulfurization.

3.4.1 Effect of temperature

Table 1 shows the effect of temperature (298-338 K) on the desulfurization of heavy crude oil using CuO nanoparticles. The results indicated that at a low temperature (298 K), the residual sulfur content was 1.664%, meaning the removal efficiency reached 6.51%, the highest value among the temperatures tested.

JOBS
مجلة العلوم الأساسية
Journal of Basic Science
Print -ISSN 2306-5249
Online-ISSN 2791-3279
العدد السادس والأربعون
٢٠٢٦م/١٤٤٨هـ

Table 1. Influence of temperature on the adsorption of sulfur compounds by CuO nanoparticles

Temperature (K)	Initial sulfur content (wt.%)	Residual sulfur content (wt.%)	Removal efficiency, R (%)
298	1.78	1.664	6.516
308	1.78	1.682	5.505
318	1.78	1.703	4.225
328	1.78	1.725	3.089
338	1.78	1.770	0.561

The results showed the best adsorption at low temperature (298 K). As temperature increased (308–338 K), adsorption efficiency gradually decreased (from 5.50% at 308 K to 0.56% at 338 K). The results indicate that adsorption is more effective at lower temperatures, and this effect diminishes with increasing temperature. This is because the temperature rises, which increases the kinetic energy of the sulfur molecules and decreases the stability of the sulfur on the surface of the CuO nanoparticles that weakens the physical/chemical attractive forces responsible for the adsorption process. The results of the present study agreed with a study done by Saod et al. (2023 [29] who stated that the adsorption efficiency is inversely proportional to the temperature. These findings agree with those of Florent et al. (2020) in their study of the adsorption of H2S onto synthetic porous materials, where the adsorption capacity decreased gradually as the temperature increased from 25 °C to 100 °C.. This was attributed to the exothermic nature of the process [30]. Similar studies using activated carbon or metal oxides have shown that adsorption decreases with temperature due to weakening van der Waals forces and a decreasing equilibrium constant.

The decrease in sulfur removal with increasing temperature can be attributed to the lower stability of adsorbed organosulfur molecules on the CuO surface. While an increase in temperature can lower the viscosity of crude-

JOBS مجلة العلوم الأساسية Journal of Basic Science
Print -ISSN 2306-5249
Online-ISSN 2791-3279
العدد السادس والأربعون
٢٠٢٦م/١٤٤٨هـ

oil and enhance the molecular mobility of the compounds, the present results indicate that this effect was offset by the weakening of the adsorbate-surface interactions and the increased tendency of sulfur compounds to desorb into the oil phase [13,16]. Moreover, the competitive adsorption of aromatic compounds, resins, asphaltenes, and nitrogen-containing species in heavy crude oil could also limit access to the active CuO sites [9,32]. However, the process cannot be described as exothermic without calculating thermodynamic parameters such as ΔG°, ΔH°, and ΔS°.

3.4.2 Effect of time

Table 2 shows the effect of contact time on sulfur removal from heavy crude oil at 25°C. The results indicate that increasing the contact time between the copper nanoparticles and the sulfur compounds gradually increased the removal ratio (R%). The removal ratio increased from 8.82% at 10 min to 21.40% at 50 min and the residual sulfur concentration decreased from 1.623 to 1.3995. This means that as time increases, the adsorption process increases, leading to higher removal levels. The removal of sulfur is done by adsorption.

Table 2. Influence of Contact Time on Sulfur Compounds Adsorption by CuO Nanoparticles.

Contact time (min)	Initial sulfur content (wt.%)	Residual sulfur content (wt.%)	Removal efficiency, R (%)
10	1.78	1.6230	8.820
20	1.78	1.5700	11.797
30	1.78	1.5250	14.325
40	1.78	1.4480	18.651
50	1.78	1.3995	21.404

When copper nanoparticles initially come into contact with sulfur compounds in crude oil, a large number of active sites on the surface of the

JOBS
مجلة العلوم الأساسية
Journal of Basic Science
Print -ISSN 2306-5249
Online-ISSN 2791-3279
العدد السادس والأربعون
٢٠٢٦م/١٤٤٨هـ

adsorbent are empty, resulting in rapid binding of the sulfur compounds due to the electrostatic attraction between the positively charged copper nanoparticles and the negatively charged sulfur particles [31]. Over time, the molecules continue to diffuse from the solution to the particle surface and occupy more of these active sites [32]. Therefore, longer contact time increases the amount of adsorbed molecules and lowers the residual concentration in the solution, reflected in higher adsorption efficiency (R%). The results of the current study are consistent with Odin's study, which confirmed that the adsorption capacity increased significantly within 20 minutes, due to two mechanisms affecting adsorption [33]. During the first five minutes of the reaction, cation exchange occurred, while the subsequent adsorption mechanism involved the formation of surface complexes in the inner shell [34]. Majid and Fakhry studied the effect of time using nickel/iodine zeolite as an adsorbent, and observed that the desulfurization process increases with time and peaks after 4 hours [35].

3.4.3 Effect of adsorbent's dose

Table ٣shows the effect of different concentrations of CuO nanoparticles 50-250 mg on sulfur removal at 298 K for 50 min. The results show that increasing the amount of CuO nanoparticle adsorbent gradually decreased the concentration of residual sulfur compounds in the solution and increased removal efficiency. At 50 mg, the removal rate was low (15.11%), then gradually increased with increasing amount, reaching 19.72% at 100 mg, 25.45% at 150 mg, 32.70% at 200 mg, and finally reaching the highest value at 250 mg, at 36.85%. This demonstrates that the adsorption efficiency improves with increasing adsorbent amount.

JOBS مجلة العلوم الأساسية Journal of Basic Science
Print -ISSN 2306-5249
Online-ISSN 2791-3279
العدد السادس والأربعون
٢٠٢٦م/١٤٤٨هـ

Table 3. Influence of Adsorbent Quantity on the Adsorption of Sulfur Compounds by CuO Nanoparticles.

CuO-NP dosage (mg)	Initial sulfur content (wt.%)	Residual sulfur content (wt.%)	Removal efficiency, R (%)
50	1.78	1.511	15.112
100	1.78	1.429	19.719
150	1.78	1.327	25.449
200	1.78	1.198	32.696
250	1.78	1.124	36.853

The results showed increased desulfurization of heavy crude oil with higher CuO-NP concentrations due to greater surface area and more effective sites for sulfur compounds. Several researchers have used nanocupric oxide to remove sulfur from model oil, but they have not applied it to heavy crude oil. However, our results are compared with previous studies to demonstrate the effect of concentration on the desulfurization process [36, 37]. Alangari *et al*., also studied the effect of adsorbent dosage on sulfur removal using a model fuel with varying amounts of CuO-NPs added, and demonstrated that the removal efficiency improved with increasing the adsorption dosage [38]. Meanwhile, Ullah et al. studied the desulfurization of model oil using activated carbon and CuO-NPs and confirmed that increasing the number of adsorbents leads to a higher removal rate [39].

3.5 Kinetic modeling

In this work, the adsorption kinetics of sulfur-containing compounds from heavy crude oil onto CuO-NPs were investigated using experimental contact-time data at 298 K. In each experiment, 20 mL of crude oil with an initial sulfur content of 1.78 wt.% was treated with 250 mg of CuO-NPs. The density of the crude oil was 0.900 g mL^{-1}. Table 4 shows the obtained adsorption capacities. The sulfur uptake increased slowly from 113.04 mg g^{-1} at 10 min to 273.96 mg g^{-1} at 50 min.

JOBS
مجلة العلوم الأساسية
Journal of Basic Science
Print -ISSN 2306-5249
Online-ISSN 2791-3279
العدد السادس والأربعون
٢٠٢٦م/١٤٤٨هـ

Table 4. Experimental adsorption capacities of sulfur compounds onto CuO-NPs.

Contact time (min)	Residual sulfur (wt.%)	Removal efficiency (%)	(q_t) (mg g^{-1})
10	1.6230	8.820	113.04
20	1.5700	11.797	151.20
30	1.5250	14.325	183.60
40	1.4480	18.651	239.04
50	1.3995	21.404	273.96

3.5.1 Pseudo first-order kinetic model

The pseudo-first order model was used to estimate the rate of sulfur adsorption on CuO-NPs. The kinetic parameters were calculated based on the linear correlation of $\ln(q_e - q_t)$ and time of contact. The pseudo-first-order rate constant was calculated from the slope of the fitted line while the intercept was used to estimate the calculated equilibrium adsorption capacity. The rate constant was 0.03154 min^{-1} and the calculated equilibrium adsorption capacity was 341.15 mg g^{-1} from the linear regression. The coefficient of determination was R^2=0.9571, this is indicating that the pseudo-first-order model was a good fit for the experimental kinetic data. However, the calculated equilibrium adsorption capacity was higher than the maximum experimental value of 273.96 mg g−1, measured after 50 min. This difference indicates that the adsorption equilibrium was probably not reached in the range of contact times studied. Thus, the calculated equilibrium capacity should be considered as an extrapolated kinetic capacity, rather than a directly obtained equilibrium capacity.

JOBS
مجلة العلوم الأساسية
Journal of Basic Science
Print -ISSN 2306-5249
Online-ISSN 2791-3279
العدد السادس والأربعون
٢٠٢٦م/١٤٤٨هـ

3.5.2 Pseudo-second-order model

The experimental contact-time data were also fitted to the pseudo-second-order model. The kinetic parameters were estimated from the linear relationship between t/qt and contact time. The slope was used to calculate the equilibrium adsorption capacity, and the intercept was used to obtain the pseudo-second-order rate constant. The equilibrium adsorption capacity was calculated to be 448.13 mg g^{-1}, and the pseudo-second-order rate constant was 6.24×10^{-5} g mg^{-1} min^{-1}. The corresponding coefficient of determination was R^2=0.8914. The pseudo-second-order model had a lower R^2 value, which indicated that the pseudo-first-order model matched the experimental data better. Moreover, the calculated equilibrium capacity was much higher than the maximum experimental adsorption capacity, further indicating that equilibrium was not reached in 50 min.

From the above analysis, the pseudo-first-order kinetic model gave a better fit than the linearized kinetic model, based on the coefficient of determination. However, the kinetics interpretation is inconclusive because the adsorption capacity continued to increase throughout the studied time interval. This means that more time must be considered to correctly estimate the equilibrium adsorption capacity and obtain reliable kinetic parameters. Below are the linearized forms of the pseudo-first-order and pseudo-second-order kinetic models for comparison purposes.

Figure 5 shows the linearized pseudo-first-order (A) and pseudo-second-order (B) kinetic models for sulfur adsorption.

JOBS
مجلة العلوم الأساسية
Journal of Basic Science
Print -ISSN 2306-5249
Online-ISSN 2791-3279
العدد السادس والأربعون
٢٠٢٦م/١٤٤٨هـ

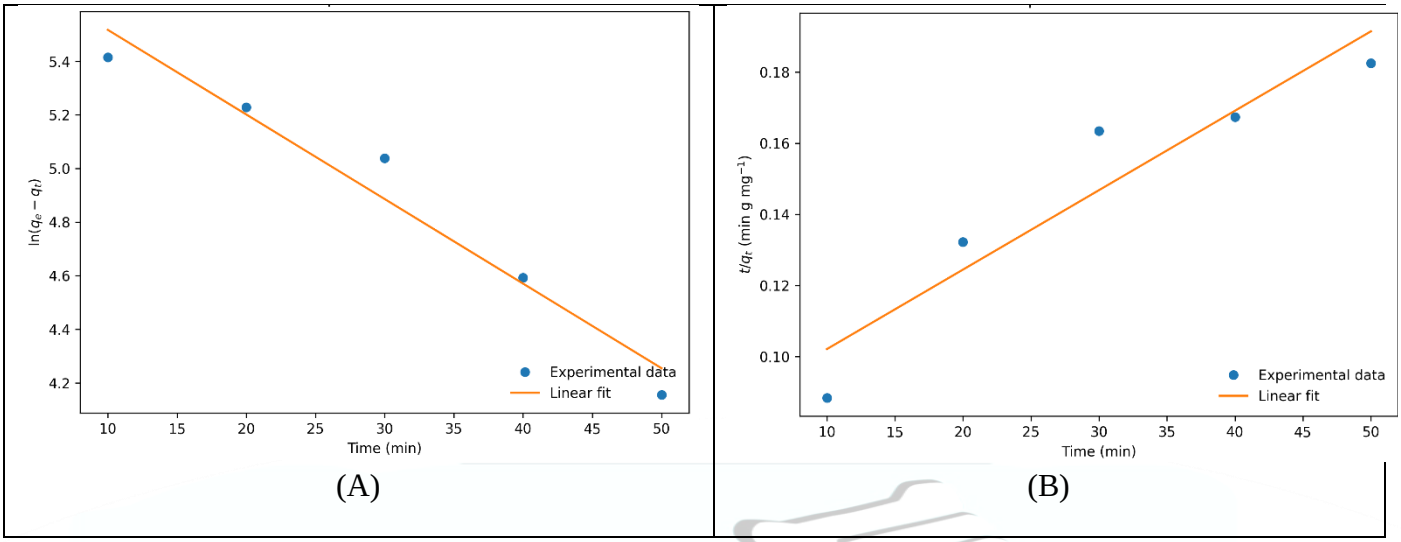

Figure 5. Linearized pseudo-first-order (A) and pseudo-second-order (B) kinetic models for sulfur adsorption from heavy crude oil onto CuO-NPs.

4. Conclusion

The synthesized CuO-NPs showed promise for adsorptive removal of sulfur compounds from heavy crude oil. Under the studied conditions, sulfur removal increased with increasing adsorbent dosage and contact time but decreased with increasing temperature. The maximum removal efficiency was 36.85 % at 298 K, 250 mg CuO-NPs, and 50 min contact time. Kinetic analysis showed that the pseudo-first-order model fit the experimental data better than the pseudo-second-order model, with R^2 values of 0.9571 and 0.8914, respectively. However, the continuous increase of adsorption capacity up to 50 min indicates that the equilibrium was not fully reached during the investigated period. Overall, the results indicate that CuO-NPs are promising adsorbents for crude-oil desulfurization. However, further work is needed before any practical application like optimization, surface-area characterization, thermodynamic analysis, longer contact-time experiments, and regeneration studies.

JOBS
مجلة العلوم الأساسية
Journal of Basic Science
Print -ISSN 2306-5249
Online-ISSN 2791-3279
العدد السادس والأربعون
٢٠٢٦م/١٤٤٨هـ

REFERENCES

1. Gounder RM. Processing of heavy crude oils: challenges and opportunities. 2019.
2. Svinterikos E, Zuburtikudis I, Al-Marzouqi M. Carbon nanomaterials for the adsorptive desulfurization of fuels. *Journal of Nanotechnology*. 2019;2019:2809867.
3. Hameed Khlaif T, Salim Bded A. Decreasing the sulfur content of crude oil by ultrasound- and activated carbon-assisted oxidative methods. In: *IOP Conference Series: Materials Science and Engineering*. IOP Publishing; 2019.
4. Pedram-Rad T, Es'haghi Z, Ahmadpour A. Adsorptive desulfurization of model gasoline using modified bentonite. *Journal of Sulfur Chemistry*. 2019;40(2):149–165.
5. Qasim A, Alwan HH. Enhancement of light naphtha quality using calcite adsorbent derived from eggshells by adsorptive desulfurization. *South African Journal of Chemical Engineering*. 2023; 46:196–204.
6. Betiha MA, Rabie AM, Ahmed HS, Abdelrahman AA, El-Shahat MF. Oxidative desulfurization using graphene and its composites for fuel containing thiophene and its derivatives: An updated review. *Egyptian Journal of Petroleum*. 2018;27(4):715–730.
7. Mguni LL, Yao Y, Nkomzwayo T, Liu X, Hildebrandt D, Glasser D. Desulphurization of diesel fuels using intermediate Lewis acids loaded on activated charcoal and alumina. *Chemical Engineering Communications*. 2019;206(5):572–580.
8. Aribike DS, Usman MA, Oloruntoba MM. Adsorptive desulfurization of diesel using activated sewage sludge: Kinetic, equilibrium, and thermodynamic studies. *Applied Petrochemical Research*. 2020;10(1):1–12.
9. Fotiadis K, Kostoglou M, Baltzopoulou P, Zaspalis V. Activated carbon modification for real diesel adsorptive deep desulfurization: Experiments and modeling. *Chemical Engineering Communications*. 2024;211(9). doi:10.1080/00986445.2024.2341265.
10. Qiu X, et al. New adsorption materials for deep desulfurization of fuel oil. *Materials*. 2024;17(8):1803. doi:10.3390/ma17081803.

11. Li T, et al. Design of porous aromatic frameworks for adsorptive desulfurization through topology-guided pore engineering. *Nanomaterials*. 2025;15(23):1815.
12. Zhu J, Zhao H, Dong X, Wang S, Hu L. Adsorption performance and mechanisms of ethyl mercaptan on Cu-impregnated hierarchical porous carbon. *Journal of Environmental Chemical Engineering*. 2025;13:120224. doi:10.1016/j.jece.2025.120224.
13. Ma L, Zhong Y, Qu L, Feng X, Zhang Y, Hou H, Yang G. Conformational flexibility of a novel Cu(I)-based adsorbent enhancing the selectivity of adsorptive desulfurization. *Separation and Purification Technology*. 2025;358:130324. doi:10.1016/j.seppur.2024.130324.
14. Hill D, Niu Y, Apsey H, Olonisakin O, Palmer RE, Alexander S. Development of $CuO/Cu_4(OH)_6SO_4$ nanoparticle mixtures to optimize H_2S adsorption. *ACS Applied Engineering Materials*. 2024;2(2):305–312. doi:10.1021/acsaenm.3c00575.
15. Musa A, Dara IA, Salisu A, Muhammad A, Saleh TA. Adsorptive desulfurization of liquid fuels over green cost-effective Cu–Ni bimetallic nanoparticles-modified alum sludge. *Nano Trends*. 2025;10:100107. doi:10.1016/j.nwnano.2025.100107.
16. Sokol HJ, Lee J, Jankovic J, Valla JA. The mechanism of adsorptive desulfurization on Cu- and Ce-exchanged Y zeolite using density functional theory. *Computational Materials Science*. 2024;235:112813. doi:10.1016/j.commatsci.2024.112813.
17. Sarkarabad KM, Shayanmehr M, Ghaemi A. Optimization and modeling of sulfur removal from liquid fuel using carbon-based adsorbents through synergistic application of response surface methodology and machine learning. *Scientific Reports*. 2025;15:4330. doi:10.1038/s41598-025-88434-1.
18. Sokol HJ, Pedram S, Jankovic J, Valla JA. Renewable activated carbon sorbent for the desulfurization of liquid fuels. *ACS Omega*. 2025;10(37):42725–42734. doi:10.1021/acsomega.5c04991.
19. Khodair ZT, Alzubaidy MWM, Almohaidi AMS, Sultan AA, Al-Shimmary SM, Albusultan SS. Synthesis of copper oxide nanoparticles (CuO-NPs) and evaluation of their antibacterial activity against *P. aeruginosa* biofilm genes. In: *AIP Conference Proceedings*. AIP Publishing; 2019.

20. Essien EA, Kavaz D, Solomon MM. Olive leaf extract-mediated zero-valent iron nanoparticles: Synthesis, characterization, and assessment as an adsorbent for nickel(II) ions in aqueous media. *Chemical Engineering Communications*. 2018;205(11):1568–1582.
21. Farouq R, Yousef N. Equilibrium and kinetic studies of copper(II)-ion adsorption onto a natural biosorbent. *International Journal of Chemical Engineering and Applications*. 2015;6(5):319.
22. Foo KY, Hameed BH. Insights into the modeling of adsorption isotherm systems. *Chemical Engineering Journal*. 2010;156(1):2–10.
23. Akintelu SA, Folorunso AS, Folorunso FA, Oyebamiji AK. Green synthesis of copper oxide nanoparticles for biomedical applications and environmental remediation. *Heliyon*. 2020;6(7).
24. Waris A, Din M, Ali A, Ali M, Afridi S, Baset A, et al. A comprehensive review of the green synthesis of copper oxide nanoparticles and their diverse biomedical applications. *Inorganic Chemistry Communications*. 2021;123:108369.
25. Vijayalakshmi R, Rajendran V. Synthesis and characterization of nano-TiO_2 via different methods. *Archives of Applied Science Research*. 2012;4(2):1183–1190.
26. Khan S, Dan Z, Mengling Y, Yang Y, Haiyan H, Hao J. Isotherm, kinetic, and thermodynamic studies of Ni and Cu adsorption by Al_2O_3 nanoparticles modified with natural organic matter. *Fullerenes, Nanotubes and Carbon Nanostructures*. 2018;26(3):158–167.
27. Manikandan B, Murali K, John R. Optical, morphological, and microstructural investigation of TiO_2 nanoparticles for photocatalytic applications. *Iranian Journal of Catalysis*. 2021;11(1).
28. Singh R, Dutta S. Synthesis and characterization of solar-photoactive TiO_2 nanoparticles with enhanced structural and optical properties. *Advanced Powder Technology*. 2018;29(2):211–219.
29. Saod WM, Alaallah NJ, Abdulkareem EA, Hilal NN, AlBiajawi MI. Effective removal of nickel and cobalt from aqueous solutions using an FeO@mSiO_2 nanocomposite. *Results in Chemistry*. 2025;13:101992.
30. Florent M, Policicchio A, Niewiadomski S, Bandosz TJ. Exploring options for improving H_2S adsorption on sludge-derived adsorbents: Formation of composites with porous carbons. *Journal of Cleaner Production*. 2020;249:119412.

31. Ahmadian M, Anbia M, Rezaie M. Sulfur dioxide removal from flue gas using supported CuO nanoparticle adsorbents. *Industrial & Engineering Chemistry Research*. 2020;59(50):21642–21653.
32. Medina OE, Céspedes S, Galindez JC, Mazo-Suarez C, Forero A, Ruiz MA, et al. Sulfur removal from heavy crude oils based on the adsorption process using CuO- and AgO-modified SiO_2-based nanomaterials: Experimental and theoretical study. *Langmuir*. 2025.
33. Uddin MK. A review of heavy-metal adsorption by clay minerals, with special focus on the past decade. *Chemical Engineering Journal*. 2017;308:438–462.
34. Chen C, Yu J, Song G, Che K. Desorption performance of commercial zeolites for temperature-swing CO_2 capture. *Journal of Environmental Chemical Engineering*. 2023;11(3):110253.
35. Dastanian M, Seyedeyn-Azad F. Desulfurization of gasoline over nanoporous nickel-loaded Y-type zeolite under ambient conditions. *Industrial & Engineering Chemistry Research*. 2010;49(22):11254–11259.
36. Ammar SH, Kareem YS, Ali AD. Photocatalytic oxidative desulfurization of liquid petroleum fuels using magnetic CuO–Fe_3O_4 nanocomposites. *Journal of Environmental Chemical Engineering*. 2018;6(6):6780–6786.
37. Sadeghi M, Yekta S, Ghaedi H, Babanezhad E. Effective removal of radioactive 90^{90}90Sr using a CuO-NPs/Ag-clinoptilolite zeolite composite adsorbent from water samples: Isotherm, kinetic, and thermodynamic studies. *International Journal of Industrial Chemistry*. 2016;7(3):315–331.
38. Alangari A, Aboul-Soud MA, Alqahtani MS, Shahid M, Syed R, Lakshmipathy R, et al. Green synthesis of copper oxide nanoparticles using the genus *Inula* and evaluation of biological therapeutics and environmental applications. *Nanotechnology Reviews*. 2024;13(1):20240039.
39. Ullah S, Hussain S, Ahmad W, Khan H, Khan KI, Khan SU, et al. Desulfurization of model oil through adsorption over activated-charcoal and bentonite-clay composites. *Chemical Engineering & Technology*. 2020;43(3):564–573.

JOBS
مجلة العلوم الأساسية
Journal of Basic Science
Print -ISSN 2306-5249
Online-ISSN 2791-3279
العدد السادس والأربعون
٢٠٢٦م/١٤٤٨هـ